A Possible Role of Water in the Protein Folding Process

Francesco Mallamace,*,†,‡ Carmelo Corsaro,‡,§ Domenico Mallamace,∞ Piero Baglioni,‖ H. Eugene Stanley,⊥ and Sow-Hsin Chen†

†Department of Nuclear Science and Engineering, Massachusetts Institute of Technology, Cambridge, Massachusetts 02139, United States

‡Dipartimento di Fisica and CNISM, Università di Messina, I-98166 Messina, Italy

§Fondazione F. Frisone, Via Etnea 73, Catania I-95125, Italy

∞Dipartimento di Scienze degli Alimenti e dell'Ambiente "G. Stagno D'Alcontres", Università di Messina, I-98166 Messina, Italy

‖Department of Chemistry and CSGI, University of Florence, Florence 50019, Italy

⊥Center for Polymer Studies and Department of Physics, Boston University, Boston, Massachusetts 02215, United States

ABSTRACT: The thermal folding of hydrated lysozyme has been investigated by means of the high resolution nuclear magnetic resonance (NMR) technique. The proton NMR signal belonging to the biomolecule hydration water (hydration level $h = 0.3$) was analyzed with the aim to explore the protein structural changes as well as to verify if water plays a role in this biological basic phenomenon. In such a way, we studied the proton chemical shift and the "apparent spin−spin relaxation time" for which water molecules assume the role of system probes in a situation in which the limited hydration of a solid-globular lyophilized protein sample (covering on average the first hydration shell) enables data interpretation devoid of complications arising from bulk water. The study was performed by means of proper temperature changes, different warming and cooling cycles, that starting from the protein in the native state explore the reversible and the irreversible phases of the denaturation. The obtained results confirm that water as a "local probe" follows accurately all the protein behaviors, detailing properly its structural and dynamical changes in this transition, from native to denatured. Since the water chemical shift, as proposed by commonly accepted theoretical and MD simulations findings, is linked to the hydrogen bond (HB) interactions, the obtained data suggest that the denaturation process is related to the average number of bonds in which the water molecules are involved.
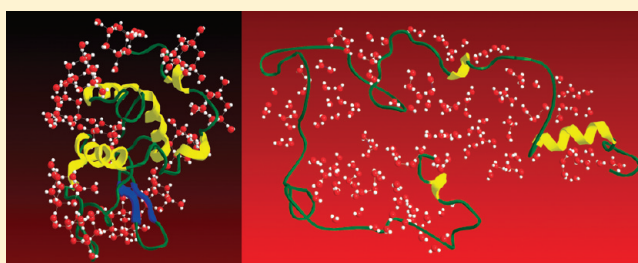
1. INTRODUCTION

The study of the structure and dynamics of water is one of the most exciting interdisciplinary research topics in science. Although it is one of the simplest molecules, water has mysterious properties that have intrigued scientists of many different disciplines and that, despite its fundamental importance in science, technology, and the environment in our daily life, are far from being completely understood and are currently under active investigation.[1−3] At the same time, proteins are considered as the major functional molecules of biology, have specific functions, and their main properties depend upon their two basic structures: the folded and the unfolded states. An essential and intriguing biological feature of proteins is the highly coherent (all-or-none) way in which these biopolymers pass forward and backward between the fully native folded state (N) and the unfolded (denatured state, D).[4] A possible reason of this reversibility is that folding has essentially three evolutionary constraints: proteins must fold to a structure in a reasonable time, the structure they fold to must perform a biological function, and the folded structure must be stable enough to perform such a function reliably. Together with the unexplained water thermodynamical properties, the protein folding ↔ unfolding process represents

today in science a deep open question: very stimulating if we consider the role of water as the "life's solvent".[5] A striking example of the biological importance of water is that proteins cannot perform their function if they are not covered by a minimum amount of hydration water, i.e., the first hydration layer.[6]

In this paper, written on the occasion of the 70th birthday celebration of Eugene H. (Gene) Stanley, who gave significant contributions to the understanding of both water and protein properties, we discuss the role of water in the protein folding ↔ unfolding thermally activated process. We essentially consider the results of different recent experiments, like nuclear magnetic resonance spectroscopy, neutron and light scattering, and calorimetry.

Protein hydration represents the process for which the incremental addition of water to the dry protein has effects on its essential properties. Beyond the first hydration layer, further addition of water does not change significantly the biomolecule

properties, resulting only in a dilution.[6−8] The hydration shell can be defined as the water associated with the protein at its hydration end point. This shell represents the monolayer coverage of the protein surface. Water outside the monolayer is perturbed to a significantly smaller extent, typically not detected by measurements of properties such as heat capacity, volume, or heat content. The quantitative dependence of protein motions on water has been illustrated, and it was established that a minimum hydration shell is required for the systems to access their functional "resilience", i.e., a dynamics state that allows biological activity.

More specifically, in a protein solution, the biomolecule interacts with two different kinds of water: (i) the bound internal water and (ii) the surface water, i.e., the H_2O molecules in direct interaction with the protein surface. The bound internal water molecules, which occupy internal cavities, seem to be extensively involved in the internal protein hydrogen bonding (HB) interaction, in the sense that water acts as a sort of glue to maintain the protein in its folded globular phase. The surface water, called the hydration water, is approximately the first layer of water molecules that interacts with the solvent-exposed protein atoms, feels the topology and roughness of the protein surface, and exhibits the slow dynamics (α-relaxation). Just the hydration water and internal water are believed to have an important role in controlling the biofunctionality of the protein.

It has been experimentally shown, by measuring over the full hydration range the reaction of lysozyme with the hexasaccharide of nacetylglucosamine, that the enzymatic activity is closely parallel to the development of surface motion, which is thus responsible for the functionality of the protein. The threshold hydration level, in this case, was measured as $h = 0.2$.[7]

Another intriguing phenomenon is the so-called protein−glass transition (or dynamic transition) observed at around $T_C = 220$ K, below which proteins show hardly any biological function;[8−10] at T_C in fact, a sharp increase in the mean square displacement $\langle x^2 \rangle$ (MSD, of both water and protein atoms) is observed. More precisely, for $T < T_C$, the protein is in a state with solid-like structure executing harmonic vibrations; as T increases above T_C, atomic motions evolve from such a state of harmonic solid to anharmonic liquid-like motions.[11] Proper experiments[10,12] and molecular dynamics (MD) simulations[13] gave evidence that this dynamic transition of proteins is solvent induced, since the hydration water also shows some kind of dynamic transition at a similar temperature.[10] In particular, Doster et al.[14] on considering infrared (IR) data suggested that the transition in the hydration water could be described as the melting of amorphous ice and that this solvent network is composed of water clusters (made of water molecules fully tetrabonded with relatively strong internal HB). They used this information to address the problem of the dynamic coupling between the solvent and the internal protein motions, suggesting that the cooperativity of the solvent HB network provides the coupling mechanism in this low T dynamical crossover. Our recent Fourier transform IR (FTIR) experiments give coherent results with such ideas suggesting that this dynamic crossover in hydration water is the result of a transition from predominantly networking water (NHB, low density) at lower temperature to partially bonded water (high density form, made of trimers, dimers, and monomers) at higher temperature,[15,16] proving that the dynamic transition of proteins is solvent-induced. More precisely, we classified water in two main bonded populations (i.e., water belonging to the HB clusters (NHB or tetrabonded) and the partially bonded (PHB)) and not bonded (free monomers). Furthermore, such FTIR results come out independently from the

hypothesis of the so-called liquid−liquid critical point (LLCP) model,[17,18] a theoretical approach developed to describe the water properties,[19] but seem to confirm previous quasi-elastic neutron scattering[20] and MD simulation experiments on the same system.[21]

It must also be highlighted that the importance of the role played by the hydration water in the protein folding behavior was well realized after the Kauzmann introduction in the literature of the "hydrophobicity", a novel concept related to the protein stability.[22] In particular, the conformational flexibility of a protein, and therefore its functionality, is extremely sensitive to the characteristics of its HBs with hydration water. This latter experimental fact is understandable considering that proteins evolved from their very beginning in an aqueous environment.

Proteins exhibit intermediate structures under denaturation (unfolding D), a process usually driven by thermal effects.[4] The dynamical properties of a protein are determined by its energetic landscape formed during the folding process. Structures in between the D and N states are unstable and contribute to an energy barrier separating the globular protein (N state) from the unfolded denatured one (D state). Whereas in the so-called kinetic hypothesis of folding the protein native structure corresponds to a relatively deep (stable) local minimum,[23] instead in the thermodynamic hypothesis such a minimum is global.[24] The highest point of the energy barrier defines the protein folding transition state (FTS). Despite the high dimensionality of the folding reaction, the FTS behaves like a transition state for a simple low-dimensional reaction, and the folding process shows simple exponential time behaviors. It follows that, in a fully reversible process D $\rightleftarrows$ N, the ratio of the rate constants (for unfolding K_u and folding K_f) is equal to the equilibrium constant: $K_{D−N} = [D]/[N] = K_u/K_f$. This, besides the complex structural composition of the FTS at microscopic level, provides a simple formalism to describe the process, allowing proper comparison between experimental observations and theory. Proteins obeying this behavior are referred to as two-state proteins. Another model of folding that properly considers hydrophilicity and hydrophobicity is the sequential one which is essentially characterized by three stages: (i) the formation of a secondary structure element, stabilized by peptide-HB, in an unfolded chain; (ii) the merging of pre-existing blocks with a secondary structure to an intermediate globular (molten) structure, stabilized by hydrophobic interactions, and (iii) the adjustment of this intermediate to the final native structure stabilized by HB and "van der Waals interactions". In all of these states, the internal water molecules are involved and can act, especially in the native globular phase, as local bridges among protein hydrophilic parts to stabilize its folded structure. Different interactions switch on consecutively, the packing increases at every step, and the highest density is reached in the native state.

Lysozyme (a small protein of 129 amino acid residues) shows intermediate structures under chemical-,[25] pressure-,[26] and thermal-induced denaturation.[27,28] As proposed by the calorimetric measurements,[27,28] its unfolding process can be considered as a three-state model: N $\rightleftarrows$ ID $\rightarrow$ D, with activation energies typical of the HB. The first step is represented by the reversible denaturation and can also be seen as a kind of strong-to-fragile liquid transition associated with the configurational entropy change,[28,29] while the second step is the irreversible denaturation and it is due to an association of unfolded lysozyme units.[26,30] All of these experimental findings have been confirmed by theory[31] and simulation.[32]

In this paper by taking into account data of previous experiments[15,20,21,34,33] and by considering a special analysis performed

at molecular level by means of the NMR technique, we discuss the physical properties of water in the thermal denaturation of proteins. The main aim of our work is to highlight the role of water in this essential biological process.

2. THE STATE OF THE ART (RECENT RESULTS)

As previously said, calorimetry is able to reveal, by a comparison between the isobaric specific heat obtained by the differential scanning calorimetry DSC ($C_{p,\text{DSC}}$) and the temperature modulated scanning calorimetry TMSC ($C_p^* = C_p' + iC_p''$), that the lysozyme thermal denaturation in aqueous solutions involves the two mentioned steps: native N $\rightleftharpoons$ ID (intermediate unfolded and possibly reversible) and ID $\rightarrow$ D (irreversibly denatured).[27] In the TMSC technique, the thermally reversible enthalpy changes are measured separately and simultaneously with the corresponding irreversible changes, showing in the C_p' vs T plot a broad peak centered at about $C_{p,\text{max}}' = 346.2 \pm 1$ K. This allows, by considering proper heating—cooling cycles, to discriminate the observed energetic situation in terms of the two processes: one, the thermal reversible contribution to C_p' and the second one that is the thermal irreversible.

In addition, such a procedure allows a precise quantitative analysis on the system thermal changes identifying the following main temperature intervals: (i) for $T < 325$ K, the initial slow C_p' increase is due to the increase in the vibrational and configurational degrees of freedom of protein native state N; (ii) for 325 K < T < 346 K, the relatively rapid specific heat increase indicates a predominant conversion of state N to state ID (with the corresponding equilibrium constant K_{D-N} that increases with T); (iii) from 346 to 356 K, the rapid C_p decrease is a result of a relatively slow increase in the amount of the intermediate state (a relatively rapid increase in post-denaturation); (iv) finally, for $T > 356$ K, a slight heat capacity increase is caused by the increase in the vibrational and configurational contributions of the denatured lysozyme, and any further denaturation. Thus, the lysozyme reversibility region stops at the end of the peak region, i.e., near 356 K.

These calorimetric results suggested us new spectroscopic (FTIR and NMR) and neutron scattering studies with the aim to explore the dynamics of hydration water in the lysozyme protein in the temperature range 180 K < T < 360 K,[15,34] also by means of proper warming and cooling cycles. Specifically, by analyzing the thermal evolution of the spectra of the OH-stretching vibration modes and the NMR self-diffusion D_S and spin—lattice relaxation time T_1, for lysozyme with the following hydration levels h = 0.3, 0.37, and 0.48, we have demonstrated the existence of two dynamical transitions in the protein hydration water. Figure 1 gives the corresponding results. In particular, the top panel (Figure 1a) represents the relative populations of the three different bonded water species. Below the first transition, at about $T_L = 220$ K, the hydration water displays the previous discussed fragile-to-strong dynamic crossover that results in the loss of the protein conformational flexibility. Above the second transition at about $T_D \simeq 346$ K (nearly equal to that of $C_{p,\text{max}}'$), where as shown by calorimetric[27] and Raman[28] experiments the protein unfolds, the dynamics of the hydration water appears to be dominated by the non-hydrogen-bonded fraction of water molecules.

Both the two dynamical crossovers are thus observable in the inverse of the NMR measured self-diffusion D_S of the hydration water molecules as a function of $1/T$ (see Figure 1, bottom left panel where D_S measured at $h = 0.3$ is compared with that of bulk water). The thermal behavior is analogous in a large temperature interval where both the water species follow a Vogel—Fulcher—Tammann (VFT or super-Arrhenius) law, $1/D = 1/D_0 \exp BT_0/(T - T_0)$. However, in the protein hydration water, the VFT behavior is observed only in the interval from T_L to T_D, where it crosses Arrhenius behavior, $1/D = 1/D_0 \exp E_A/RT$. Thus, in the very low and in the very high temperature regimes, hydration water follows a two-stage thermally activated energetic behavior, and specifically the high-temperature data behavior can be fitted with $E_A = 5.97 \pm 0.55$ kcal/mol, which corresponds to about an energy needed to break 2.4 hydrogen bonds at T_D.[35]

More precisely by means of the FTIR spectroscopy, we have considered the experimental OH stretching (OHS) vibrational spectra of lysozyme hydration water, whereas with the NMR we have investigated the long-time diffusion of both high and low temperature dynamic crossover phenomena. Both the crossovers are observable by means of the neutron scattering by measuring the hydration water mean square displacement, the average relaxation time, and the self-diffusion coefficient.[8,20,33,36] In particular, because NMR measures the long-time millisecond self-diffusion constant, during which the water molecules may have reached the boundary of the confinement and reflected back, we have also considered the quasielastic neutron scattering (QENS) that measures D_S on a subnanosecond scale. We also have profited of the QENS technique to extract the migration distance d of the hydration water, observing a pronounced increase in such a quantity above T_D.[33]

The low-temperature FSC dynamic crossover transition at about 225 K is also related to the protein " glass" transition which, according to the neutron scattering data on the FSC,[9,10,20] is triggered by the strong coupling between the protein and the hydration water. However, the main result of our FTIR experiments which focus on water dynamics is that both protein transitions are connected to the change of local hydrogen bond pattern which in turn leads to mobility changes of both the hydration water and the protein. Whereas at the low temperature crossover there is a change in the water population from water molecules belonging to the HB network to mobile water (partially bounded and free), at the second crossover T_D, the majority of water molecules are free.

More information on the dynamics of hydration water in the high-temperature crossover has been obtained by means of the NMR proton spin—lattice relaxation time T_1 measured under the same experimental conditions as the self-diffusion experiment (Figure 1, bottom right panel). T_1 represents the longitudinal relaxation time of protons and as it is well-known is connected, together with the spin—spin proton transverse relaxation time T_2, to the transport properties of the system.[37] The hydration water spin—lattice relaxation time is characterized by two contributions, one coming from the hydration water protons (order of seconds as in bulk water) and the other one from the protein protons (of the order of 10 ms). The figure also shows that, on the contrary of bulk water (a VFT behavior), the hydration water T_1 is characterized by two different temperature behaviors above and below the onset of the reversible unfolding regime. In the protein N state, the hydration water longitudinal relaxation time increases with T, following a behavior that is similar to that of bulk water, whereas that of the protein protons remains nearly constant. The situation changes dramatically on approaching T_D and the region of the high-temperature protein dynamical transition where the T_1 of the protein protons drops abruptly and disappears just at T_D. Conversely, the T_1 of hydration water
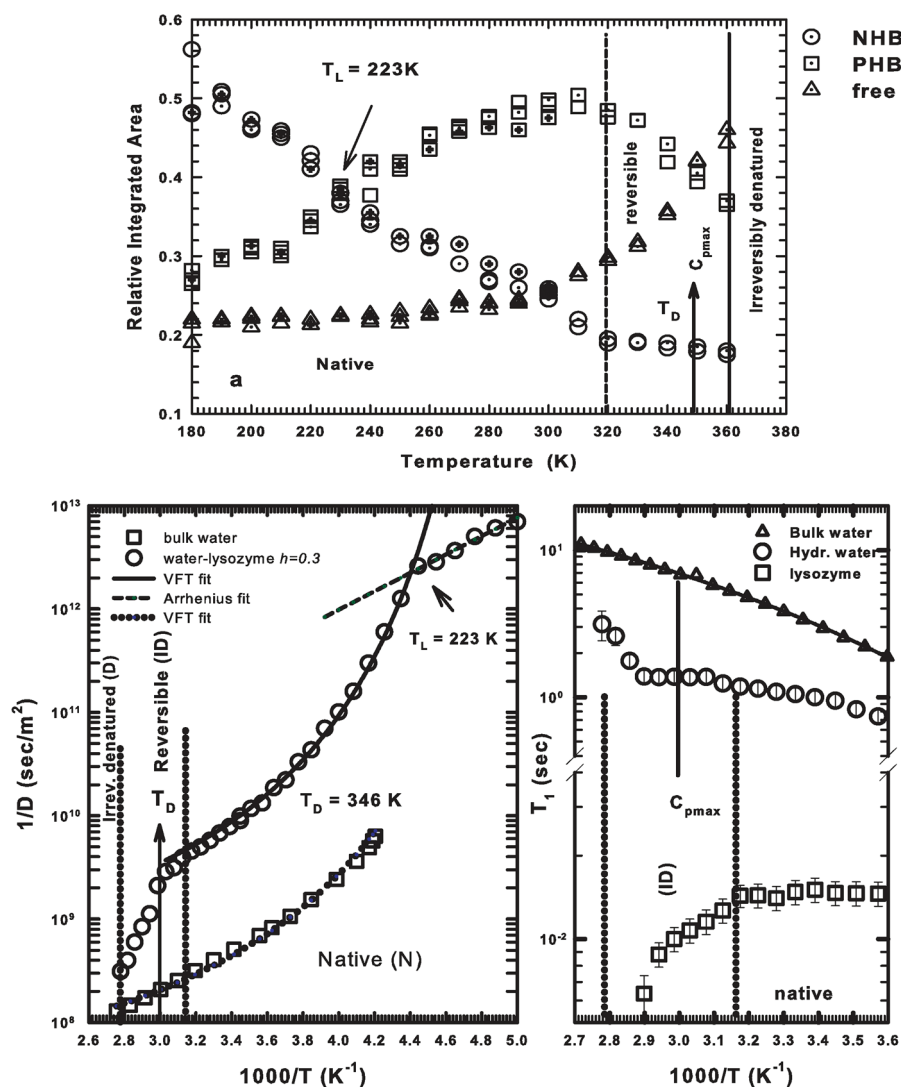
Figure 1. (top panel) The relative populations of the three different bonded water species at the different temperatures. As it can be seen, the two crossovers take place when a species becomes dominant with respect to the others. (left panel) The inverse of the NMR self-diffusion coefficient D_S of the lysozyme hydration water molecules as a function of $1/T$, for $h = 0.3$, compared with that of bulk water. (right panel) The NMR proton spin−lattice relaxation time constant T_1 measured under the same conditions. Both quantities show a clear dynamic crossover at T_D, and after it, their behavior evolves toward that of bulk water, crossing it at about its boiling point. According to the specific heat results, the main regions of the folding process are indicated together with the native one.[27]

remains nearly constant, and afterward it shows a sudden increase toward the values of bulk water, before irreversible denaturation intervenes (a behavior analogous to that of the self-diffusion coefficient, Figure 1, bottom left panel). In summary, also in the high temperature region, there is an overall agreement between the NMR data and the FTIR OHS vibrational spectra. The protein denaturation process, accompanied by an early stage of reversibility, starts just when the population of free molecules approaches that of the bonded, i.e., just when the probability for water molecules to form a HB is about the same as it is to be nonbonded.

The theory predicts that slope changes in the Arrhenius plot of the inverse of the diffusion coefficient take place when the configurational contribution to the specific heat has a maximum, and it is known that the Adam−Gibbs equation relates these quantities as[38]

$$\frac{1}{D} = \frac{1}{D_0} \exp\left(\frac{C}{TS_{\text{conf}}}\right) \tag{1}$$

where $1/D_0$ is a prefactor, C is a constant, and S_{conf} is the system configurational entropy. It is thus clear that by assuming the validity of this latter equation the specific heat peak characterizing the lysozyme thermal denaturation is associated with the existence of a high-temperature crossover phenomenon in the inverse of the diffusion constant of the hydration water. These results were confirmed also by means of special NMR measurements[34] where it has been found that the contribution of the configurational disorder to entropy is dominant, so $S_{\text{conf}} \approx S$ and

$$S_{\text{conf}}(T) \approx S_{\text{conf}}(0) + \int_0^T \frac{C_p}{T} \, dT \tag{2}$$

These NMR results come out from the fact that the proton chemical shift, δ, of water is directly connected with the magnetic shielding tensor, and thus represents the local hydrogen-bond geometry and order.[34] More precisely, there is a large literature[39−41] showing direct relation between $\delta(T)$ and the average number of

14283

dx.doi.org/10.1021/jp205285t |*J. Phys. Chem. B* 2011, 115, 14280−14294
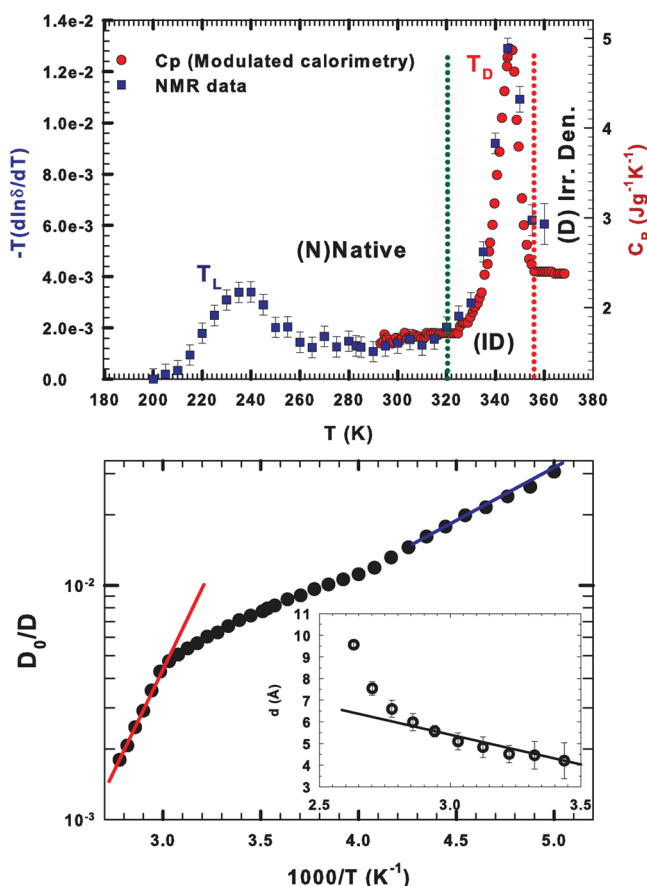
Figure 2. (upper panel) The temperature derivative of the NMR fractional chemical shift (left axis) and the specific heat measured by TMSC (right axis) as a function of T, for the water/lysozyme system. (lower panel) Arrhenius plot of D_0/D vs $1000/T$ calculated according to the Adam−Gibbs equation by considering the NMR chemical shift data. Note the agreement with change in the slope for the inverse of the diffusion constant at 340 ± 5 K shown in Figure 1. (inset) The experimentally extracted average migration distance d of the hydration water (QENS experiments) slowly increases linearly within experimental error bars below T_D but rises sharply above T_D, indicating a longer migration of water molecules in between two successive trap sites.[33]

HBs, $\langle N_{HB} \rangle$, in which a water molecule is involved, $\delta(T) \propto \langle N_{HB} \rangle$. Since $\langle N_{HB} \rangle$ is related to the number of possible water configurations, one can assume $S_{conf} \approx -K_B \ln\langle N_{HB} \rangle$. Therefore, the temperature derivative of the measured fractional chemical shift

$$-\left(\frac{\partial \ln \delta(T)}{\partial T}\right)_P \approx -\left(\frac{\partial \ln\langle N_{HB} \rangle}{\partial T}\right)_P \approx \left(\frac{\partial S_{conf}}{\partial T}\right)_P \qquad (3)$$

should be proportional to the constant pressure specific heat $C_{p,conf}(T)$ (being $C_P = T(\partial S/\partial T)_P$). Such a quantity was measured in these terms for confined water in silica nanotubes in the very supercooled regime and in lysozyme hydration water in the temperature range 195 K < T < 350 K.[34] Figure 2 (upper panel) shows, in a double scale plot, $(-T\partial \ln \delta(T)/\partial T)_P$ for lysozyme hydration water, whereas in the right-hand side C_p measured by means of the TMSC technique is reported. One can see that $(-T\partial \ln \delta(T)/\partial T)$ displays two maxima. The first, never experimentally measured in the deep supercooled regime below 250 K for water, is observed for both types of confined water at the

temperature of the first dynamical crossover. The second instead is observed at a temperature nearly coincident with the associated protein denaturation process (i.e., at the second dynamical crossover). Figure 2 (lower panel) reports the Arrhenius plot of D_0/D vs $1000/T$ calculated according to the Adam−Gibbs equation by considering the NMR specific heat (chemical shift data), a plot in agreement with the data of Figure 1 (a change in the slope for the inverse of the diffusion constant at 340 ± 5 K). In the inset, the experimentally extracted average migration distance d of the hydration water (QENS experiments) is reported; this quantity is slowly increasing linearly within experimental error bars below T_D but rises sharply above T_D, indicating a longer migration of water molecules in between two successive trap sites.[33]

This is the actual situation regarding the lysozyme folding−unfolding process coming out from a series of different experiments and in some way confirmed by MD simulations.[13,21,33,36] We presume that the role of water, and in particular of the HB between water−protein and water−water needs some additional studies especially from a local point of view. On these bases, we have considered new NMR studies made just on the behavior of the proton chemical shift (PCS) of the water−lysozyme system (with $h = 0.3$) in different thermal cycles covering the principal intervals, as proposed by the TMSC experiment, of the process $N \rightleftarrows ID \rightarrow D$.

3. METHODS

3.1. Hydrated Protein Preparation. Hen egg white lysozyme used in this experiment was obtained from Fluka (three times crystallized, dialyzed, and lyophilized) and used without further purification. Samples were dried, hydrated isopiestically, and controlled by means of a precise procedure.[20] We used samples with the same hydration level $h = 0.3$.

The sample was lyophilized overnight to remove any water left (about 7%). The dried protein powder was then hydrated isopiestically at 5 °C by exposing it to water vapor in a closed chamber until a hydration level of $h = 0.30 \pm 0.01$ was reached, i.e., 0.30 g of water/g of dry lysozyme. The hydration level was determined by thermogravimetric analysis and also confirmed by directly measuring the weight of the absorbed water. This hydration level was chosen to have about a monolayer coverage on the protein surface. For each experimental run, we have used different samples.

3.2. NMR Experiments. The dynamical properties of the system lysozyme−hydration water have been studied at ambient pressure and different temperatures by using a Bruker AVANCE NMR spectrometer operating at 700 MHz ^{1}H resonance frequency. In these NMR experiments, we have focused our interest in the ^{1}H NMR spectra (obtained from the free-induction decay (FID)) by measuring the proton chemical shift, the maximum intensity I^{max} (or $I_{NMR}(T)$), and the apparent spin−spin relaxation time T_2^* (a quantity related to the proton rotational time, i.e., a measure of the interparticle orientational time). We have explored the hydrated protein as a function of the temperature in proper heating−cooling cycles with an accuracy of ± 0.2 K by using the T-dependence of the chemical shift of ethylene glycol as a T standard. The spectroscopic experimental configuration was the "magic angle spinning (MAS)". By tilting samples of a precise angle (about 54.7°) with respect to the direction of the applied magnetic field, the Hamiltonian term corresponding to dipolar interactions vanishes and NMR peaks become narrower.[42] Hydrated protein powders were placed in a 50 μL rotor and

spun at 4000 Hz at the magic angle to increase the spectral resolution.

We have conducted the experiments by means of different heating—cooling cycles exploring completely or partially the folding process N $\rightleftarrows$ ID $\rightarrow$ D. In particular, these cycles are the following: (i) in the cycles A and B all the folding process was studied, in the A case the hydrated lysozyme was heated from 295 to 365 K and than cooled up to 297 K, whereas in the B cycle the covered range was the following: heating from 296 to 366 K and than cooling up to 298 K. In both the warming and the cooling cycles, the proton chemical shift has been measured with steps of $\Delta T = 2$ K; (ii) in the C and D cycles, we have worked inside the N $\rightleftarrows$ ID region, in both we have started with the sample heating at 320 K with the difference that in the C case the cycle was inverted just to near after T_D (i.e., 347 K) whereas in D cycle the cooling was initiated at 343 K, just 3 K before the temperature of the maximum in the specific heat T_D; (iii) cycles E and F, here we have operated by performing a system annealing at a certain temperature inside the cooling part of the cycle (specifically in the region N $\leftarrow$ ID), in both cases starting from 320 K we have reversed the temperature at 341 K, but at 330 K the thermal cycle was stopped by maintaining T constant and performing the PCS measurements with intervals of 1 h up to 20 h in the E case and for 28 h in the F case; (iv) finally the cycle G operating only inside the native N state was explored. Each heating or cooling step ($\Delta T = 2$ K) was made slowly in about 20 min just to avoid unwanted abrupt temperature variation.

3.3. Chemical Shift. The chemical shift δ is an assumed linear response of the electronic structure of a system under investigation to an external magnetic field B_0, as $B(j) = (1 - \delta_j)B_0$, where j is an index identifying the chemical environment.[43,44] Specifically, δ is related to the magnetic shielding tensor σ, which in turn relates to the local field experienced by the magnetic moment of the observed nucleus. The magnetic shielding tensor σ, strongly dependent on the local electronic environment, is a useful probe of the local geometry; and in particular for the hydrogen bond structure for water and aqueous systems and solutions.[45] Of interest are generally its isotropic part, $\sigma_{iso} \equiv \mathrm{Tr}(\sigma/3)$ and anisotropy $\Delta\sigma \equiv \sigma_{33} - (\sigma_{11} + \sigma_{22})/2$ (σ_{11}, σ_{22}, and σ_{33} being the three principal σ components); σ_{iso} is experimentally obtained via the measured δ relative to a reference state through the relation $\delta = \sigma_{iso}^{ref} - \sigma_{iso} + (A - 1/3)(\chi^{ref} - \chi)$. Here, χ is the magnetic susceptibility and the factor A depends on the sample shape and orientation; $A = 1/3$ for a spherical sample. Since the magnetic field exerted on a proton is $B_0[1 + (4\pi/3)\chi(T)]$, the resonance frequency is $\omega(T) = \gamma H_0[1 - \sigma(T) + (4\pi/3)\chi(T)]$, where γ is the proton gyromagnetic ratio. Thus, the deviation of $\sigma(T)$ from a reference value gives $\delta(T)$. Since the magnetic susceptibility per water molecule, χ_0, can be assumed to be T and P independent, $\chi(T)$ is simply given by $\chi_0\rho(T)$, where $\rho(T)$ is the density at a temperature T.

In the liquid and gas phases, $\omega(T)$ and $\rho(T)$ can be obtained directly from the experiment. Considering that water molecules in the gas phase at 473 K are isolated, we can set $\delta_g(473\ \mathrm{K}) = 0$, where g indicates the gas. Thus, $\delta(T) = [(\omega(T) - \omega_g)/\omega_g - (4\pi/3)\chi_0(\rho(T) - \rho_g)]$. In such a way, $\delta(T)$ can be determined from $\omega(T)$ and $\rho(T)$. Hence, an isolated water molecule in a dilute gas can be taken to be the reference for δ, so that δ represents the effect of the interaction of water with the surroundings, providing, in particular, a rigorous picture of the intermolecular geometry.[39] In liquid water, the shielding tensor is isotropically averaged by fast molecular tumbling, so the NMR

frequency provides information only on σ_{iso}. In addition, the $\Delta\sigma$ contribution escapes detection because ^{1}H relaxation is heavily dominated by the strong magnetic dipole field from nearby protons.[46]

As we have mentioned above, δ is directly related to the average number of hydrogen bonds in which a water molecule is involved.[39−41] Furthermore, with the NMR signal intensity $I_{NMR}(T)$ being directly related to the system equilibrium magnetization M_0 (or the susceptibility χ_0), which depends linearly on the total number of mobile spins per unit volume, on the mean square value of the nuclear magnetic moment, and on $1/T$ (Curie law), the obtained NMR spectra were corrected for the Curie effect.

4. RESULTS AND DISCUSSION

4.1. The Spectral Evolution. The ^{1}H NMR spectra (obtained from the FID) of hydrated lysozyme measured in cycle A upon the warming and cooling phases are shown in a three-dimensional plot in Figure 3a and b, respectively. Figure 3a displays well the evolution from the native to the unfolded state. The intense contribution (4 orders of magnitude higher) centered at about 4.5 ppm belongs, as it is well-known, to water and thus in our case to the hydration water protons, whereas the other peaks belong to protein protons. In the low T regime, as it can be observed, these latter are almost completely smeared out, meaning that protein side chains are not mobile on the NMR time scale at this hydration level. The situation changes at about 325 K, above this temperature, which is on the border between the native and the intermediate region, and protein side chains increase their mobility. Furthermore, on increasing the temperature and in particular above 346 K, clear and more resolved peaks appear in the spectra. These contributions belong to the protein side chains and as it can be observed, by increasing the temperature, are characterized by a progressive narrowing in their width, a process that as it is well-known is associated with an increased mobility of the system. Figure 3b illustrating the spectral evolution during the cooling gives evidence of the irreversibilty, showing that the protein side chains maintain a certain mobility also at the low, end cycle, temperatures.

At this stage, making reference to our main objective, i.e., the clarification of the role of water on the protein denaturation, we considered as an operating strategy to treat only the water proton contribution on these ^{1}H NMR spectra. The next figure (Figure 4) thus illustrates the thermal evolution of the water protons signal during some characteristic warming—cooling cycles. More precisely, the left side of Figure 4a deals with cycle A which explores a temperature range that covers all three regions: native, intermediate (reversible) denaturation, and irreversible denaturation, whereas the right side of Figure 4a deals with cycle G that works only in the protein native region. A first inspection of these data clearly evidences the absolute irreversibility of cycle A, whereas cycle G appears essentially reversible. Both cycles are characterized by changes in the corresponding spectral contributions, like the intensity (I), the shift of the central frequency value (or chemical shift, δ), the shape, and the HWHM peak width, $\Delta\nu$ (that can be used to obtain the apparent spin—spin relaxation time of water protons directly, being $T_2^* = 1/(\pi 2\Delta\nu)$). Just these changes as a function of the temperature can give answers to our question.

Figure 4b characterizes what happens inside the intermediate region explored with two thermal cycles D (left side) and E (right side) starting both from the native protein phase but completely

14285

dx.doi.org/10.1021/jp205285t |*J. Phys. Chem. B* 2011, 115, 14280–14294
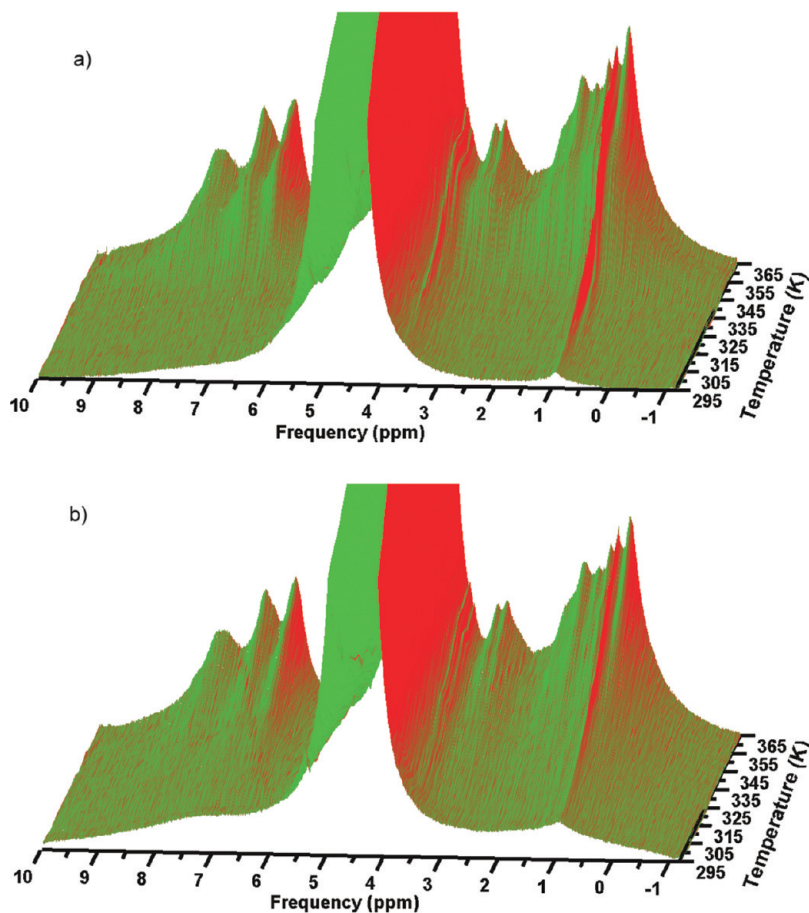
Figure 3. ^{1}H NMR spectra (obtained from the FID) of hydrated lysozyme measured in cycle A upon the warming (a) and cooling (b) phases, shown in a three-dimensional plot.

different in their thermal evolution. As previously specified, the first case (D) starting from the N state at 320 K is characterized by a warming stop just 3 K before the temperature of the maximum in the specific heat T_D (i.e., 343 K); after that, the thermal cycle was inverted, returning to the starting temperature. Whereas the second illustrated cycle (E) is characterized by the thermal annealing, more precisely by operating at about the same temperatures of the previous one the cooling was started at $T = 340$ K and stopped at 330 K; after that, the temperature was maintained constant for a period of 20 h in which the PCS measurements have been performed with intervals of 1 h. In the final stage of the latter case, the onset of the protein denaturation is evident. In addition, in both cases, inside this intermediate region and thus near the $C'_{p,max}$ temperature, there are clear signs of the irreversibility, a situation that appears in some aspects different from that proposed by the TMSC calorimetric study.[27] According to this latter study, it seems that the annealing process will result in the protein denaturation, but on the contrary, our NMR data propose that the ID region includes also the region in which is located the specific heat maximum. In summary, our data indicate that the borderline between the ID → D process is represented just by such a maximum at T_D.
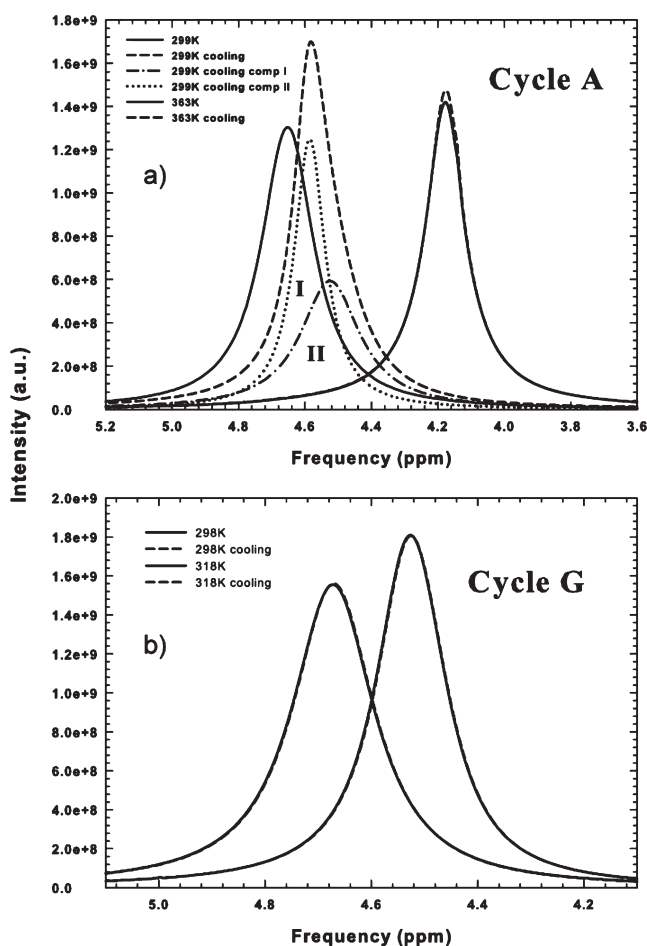
The spectral transfer function of the NMR instrument is typically represented by a Lorentzian form so that it is customary to analyze the corresponding measured spectra by means of this function. Figure 5 well illustrates such a situation; as it can be easily observed, in the case of cycle G (the one performed inside

the native protein phase, N), all the spectra during the warming and cooling processes can be described by the use of only one Lorentzian form; instead, the final part of the heating phase of cycle A and all its cooling parts are characterized by strong spectral changes. It is evident from this that such an approach furnishes a correct experimental procedure to test the level of reversibility in the protein folding process looking only to the hydration water. More precisely, the absolute reversibility will be proved only when, within the experimental error, the same Lorentzian (i.e., same parameters: chemical shift (δ), intensity, and HWHM $\Delta\nu$) fits the two ^{1}H NMR spectra measured respectively at the same temperatures inside the heating and cooling phases of a certain cycle.

The absolute reversibility of thermal changes in the native phase is just quantitatively proved by this. Well different is, instead, the situation observed in the cycle A where the exploration was extended well inside the region of the protein irreversible denaturation (Figure 5a). In such a case, the irreversibility is complete and evidenced by strong spectral changes in form, intensity, and δ. In particular, Figure 5a illustrates that the measured spectra at the end of the cycle ($T = 295$ K, cooling) can be analyzed only by means of two different Lorentzians, named I and II. Because these two latter contributions appear just after the crossing of the border of the ID → D phases, we have assumed that the denaturation coincides with the possibility to detect both the external protein hydration water and the internal one. When proteins unfold in an open polymeric structure, the
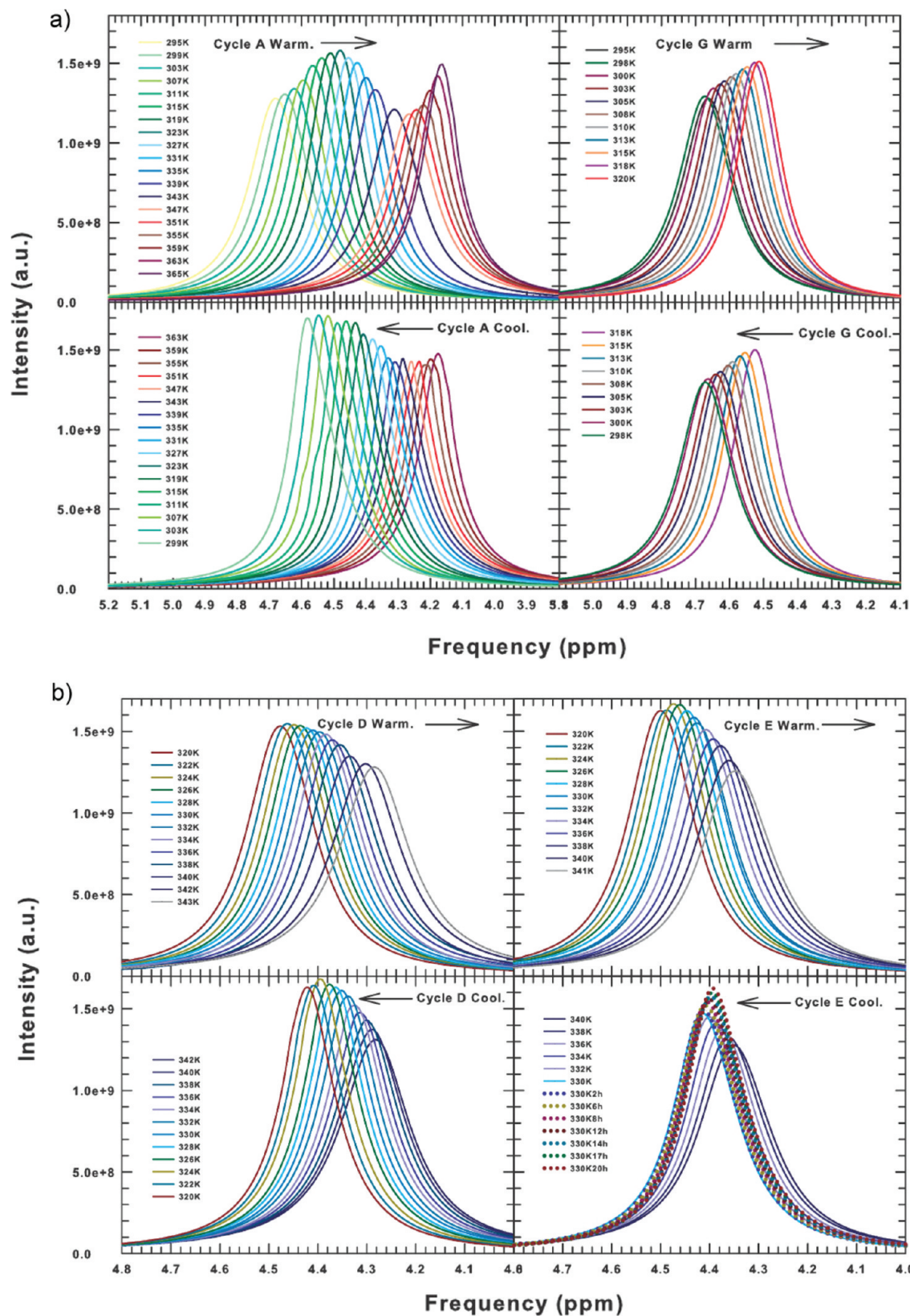
Figure 4. The thermal evolution of the NMR signal of the water protons during some characteristic warming—cooling cycles. (a, left side) Cycle A covers all three thermal regions: N, ID, and D; (a, right side) cycle G works only in the protein native region N; (b, left side) cycle D starts from 320 K up to 343 K and cooling back; (b, right side) cycle E starts from 320 to 340 K and cooling back up to 330 K where we have performed a PCS measurement with intervals of 1 h up to 20 h.

Figure 6. (A) NMR proton spectral intensities, $I_{NMR}(T)$, during the warming phase for all cycles and also during the cooling phase only in the case of the reversible cycles. (B) $I_{NMR}(T)$ in the cooling phase of the irreversible cycles.

Figure 5. (a) Representative spectra of cycle A shown as the irreversibility of the process is complete and evidenced by strong spectral changes in form, intensity, and δ. In particular, the measured spectra at the end of the cycle (T = 295 K, cooling) are fitted by two Lorentzian components (I and II). (b) All the spectra acquired during the warming and cooling processes of cycle G (the one performed entirely inside the native state) can be described by the use of only one Lorentzian and demonstrate as the process is totally reversible.

internal water (also considering the effective high temperature) can easily break the HBs that link it to the protein residuals and can diffuse and interact with the external one. This reason explains the presence of two proton water NMR signals inside the phase D. Whereas the component II is related with the internal water, the component I belongs again to the external one. A support on such a picture is given by the mentioned FTIR results,[15] that relate the relative integrated areas of the OHS components essentially with the PHB and the free water species, areas which cross just near T_D, i.e., just when the probability for water molecules to form a HB (or more explicitly the HB lifetime) is about the same as that to be nonbonded. As mentioned above, after the denaturation, these two water forms are present in the system and can interact with each other or with the open biopolymer, in a complete different physical scenario if compared with the folded protein native state. We hope to clarify it, illustrating soon the thermal evolution of the intensities (more precisely the value at the spectral maximum $I_{NMR}(T)$) (Figure 6), the apparent spin−spin relaxation times T_2^* (Figure 7) and the chemical shifts (Figure 8), extracted by the NMR water proton
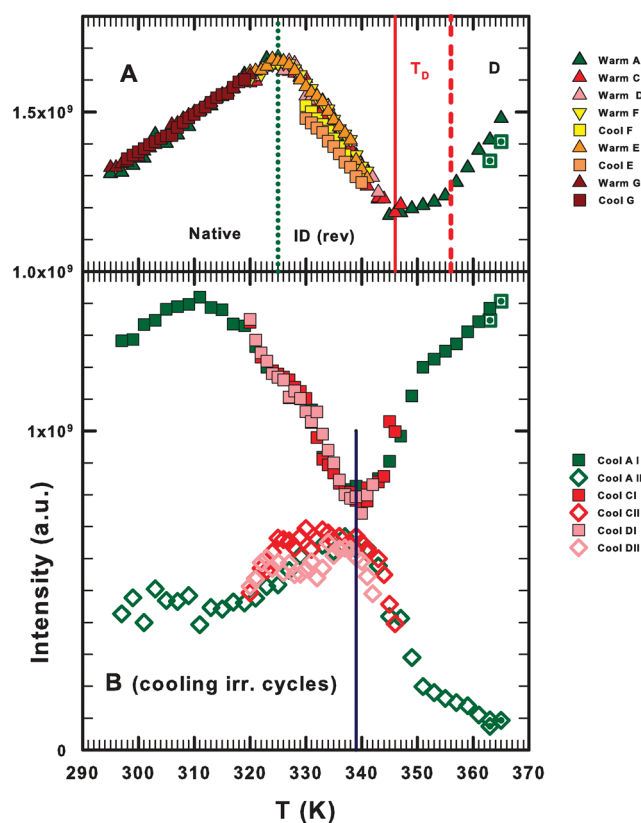
spectra measured here. Finally, we will report the configurational specific heat extracted according to our NMR procedure[34] (Figure 9). On looking at Figures 4 and 5 (especially the cycle A spectra), one can easily observe that an increase in the spectral intensity corresponds to a frequency narrowing and vice versa. This means that the intensity and the spin−spin relaxation time can have analogous thermal behavior; this is in fact reflected, as it is observable in part A of Figures 6 and 7, by their overall evolution in the warming phase.

Just to have a clear data representation, we have considered plotting separately, in the case of the intensity and the relaxation times, the warming and cooling parts of each cycle; only in the case of the reversible cycles both the warming and cooling data are all arranged in the same plots (part A of Figures 6 and 7). The coolings of the irreversible cycles are reported in part B of the corresponding figures. Figure 6 illustrates as a function of the temperature the proton spectral intensities, $I_{NMR}(T)$, or the system equilibrium magnetization M_0 (related to the molecular magnetic susceptibility χ_0 and proportional to the atomic concentrations), after the Curie law corrections. For proper data identification, we have considered (for this one and the next figures) different colors for the different cycles with different symbols for the warming (triangles) and cooling phases. We also reported, when present, the spectral contributions I (squares) and II (diamonds).

It must be stressed that what we observe, in these warming phases, is entirely due to the contribution to the ^1H NMR spectra of all the protein hydration water until the protein starts to unfold,
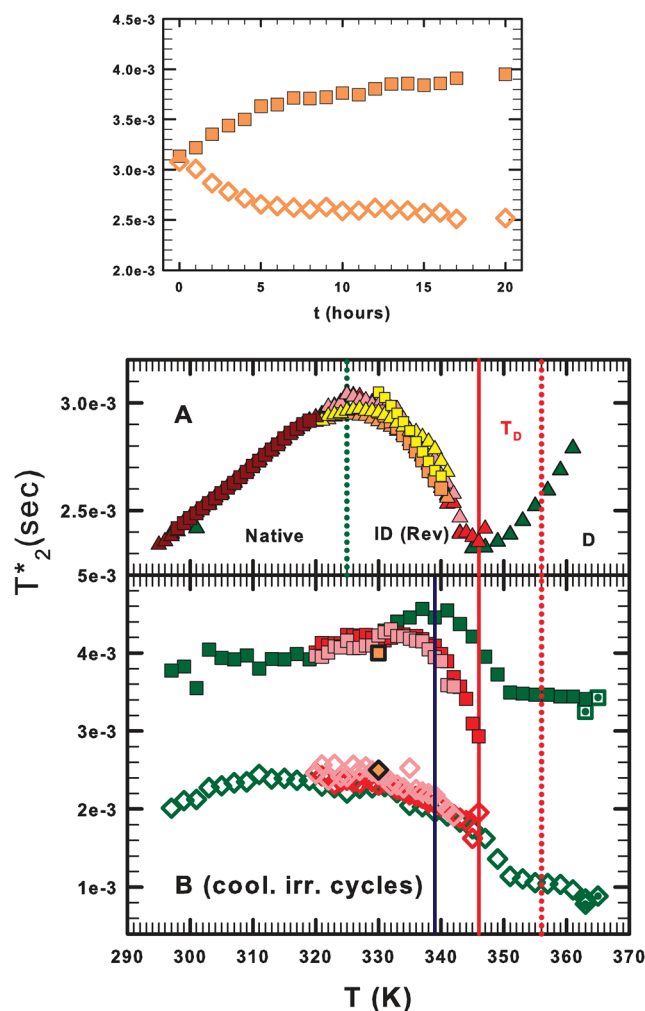
Figure 7. (upper panel) The temporal evolution of the apparent spin—spin relaxation time T_2^* of the two contributions measured during the isothermal annealing (at $T = 330$ K) of cycle E. (A) T_2^* during the warming phase for all cycles and also during the cooling phase only in the case of the reversible cycles. (B) The same as part A but during the cooling phase of irreversible cycles. One can note that, in the case of cycle A, the T_2^* corresponding to contribution I evidences a maximum just at around $T \simeq 340$ K, whereas the one corresponding to contribution II is characterized by a slow evolution toward a stationary behavior at the lowest temperatures.

a condition in which the internal water cannot give any spectral contribution, being essentially frozen in the biopolymer structure.

In the warming phase (see Figures 6 and 7), we have in the magnetization $I_{NMR}(T)$ and in the spin—spin relaxation time $T_2^*(T)$ similar temperature behaviors with two crossovers coincident with the special temperatures characterizing the protein behavior as evidenced by the specific heat data:[27] the first one is coincident with the temperature $T = 325$ K, the N $\rightleftarrows$ ID transition locus (reported as a dotted line), and the second one is observed at about $C_{p,max}'$ (i.e., T_D, continuous line). More precisely, the spectral intensity and the relaxation time increases, by increasing T, up to $T = 325$ K; after that, it starts a decrease that ceases with a minimum at about T_D, where a new growth restarts.

An overview of the strong link between hydration water and the protein during the unfolding process can be accounted for by

considering, together with these NMR and C_p findings, the FTIR results (Figure 1, top panel). In particular, these data stress that, at these high temperatures of the unfolding, the PHB water molecules have strong influences on the native protein phase, whereas the water monomers seem to dominate the irreversible denaturation one. In fact, we observe that the temperature where the PHB water population has its maximum coincides with the $I_{NMR}(T)$ and $T_2^*(T)$ maxima ($T \sim 325$ K), whereas their minima mark the crossover temperature ($\sim T_D$) at which monomers represent the majority of the water molecules. More complex it appears the situation in between these maxima and minima marking, respectively, the N $\rightleftarrows$ ID transition (or the unfolding beginning) and the borderline of the folding reversibility. Meaning that whereas below 325 K the protein interacts essentially with its hydration water, above such a temperature are also available interactions between the protein hydration and internal water in an increasing manner by increasing T. Above the temperature of the maximum in the specific heat T_D (i.e., 346 K), there is the onset of the protein irreversible denaturation with a complete structural change in the biopolymers that allows the water (hydration and internal) to interact not only with the hydrophilic but also with the hydrophobic protein groups with sudden effects in the proton dynamics.

The presence of a minimum in both $I_{NMR}(T)$ and $T_2^*(T)$ is explained by the fact that the starting in the unfolding process is accompanied by an increasing in the system configurational changes as revealed by the NMR and neutron diffusion measurements and by the specific heat behavior. This simply means an increase in the system degrees of freedom that is reflected essentially in both the average proton magnetization and relaxation times and thus also in the averaged HB numbers. The effect of this latter situation constitutes the final part of this work where we will study the behavior of the proton chemical shift. We also remember that $T_2^*(T)$ is a quantity connected with a sort of average rotational proton relaxation time,[37] i.e. a quantity strongly linked with the system local changes. On these bases, a maximum in the configurational energy behaves as a minimum in the two quantities that are the object of our discussion (magnetization and spin—spin relaxation time).

From a molecular point of view, the increasing amount of the water monomer seems to also be the effect of a more dynamical system situation reflected by a knee, located at around T_D, in the configurational entropy calculated by the calorimetric data.[33] The T_D region, where the PHB and free water concentrations cross, can be considered as a metastable region where the protein can fold; here in fact the HB breaking becomes highly probable, not only for water but also for the protein. Therefore, such a sharp change in S_{conf} may be considered as the sign of the onset of the irreversible denaturation.

As previously said above T_D, protein goes quickly toward the structural phase of an open polyelectrolyte, offering to the solvent, composed now by hydration and internal water, both the hydrophilic and hydrophobic parts and a sudden T increase above T_D will cause the irreversible denaturation.

As illustrated by Figure 5, when the protein unfolds irreversibly, the situation changes completely and the first signal we have is that the NMR spectra cannot be treated by the use of only one Lorentzian component. We need now two components that can be related to the new forms of the polyelectrolyte "solvation" forms. Figure 6B illustrates this latter situation: just when the temperature of cycle A is inverted ($T = 365$ K), we need to treat the NMR spectra with two spectral contributions, one with a
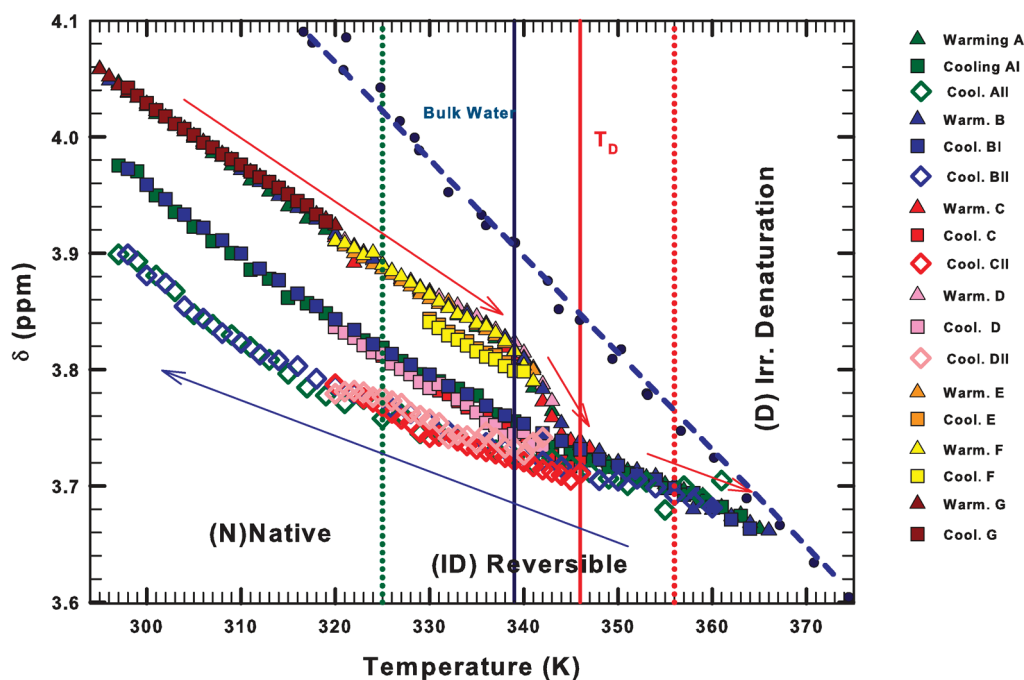
Figure 8. Thermal evolution of the measured ^1H NMR chemical shift $\delta(T)$ for all the studied thermal cycles. For comparison, the data of the pure bulk water chemical shift are also reported. Note that the analytical continuation of the measured protein hydration water $\delta(T)$, corresponding to the warming phase at the highest temperatures, crosses the pure bulk water chemical shift at about 370 K. The same situation was found for the self-diffusion coefficient and spin−lattice relaxation time (see Figure 1).
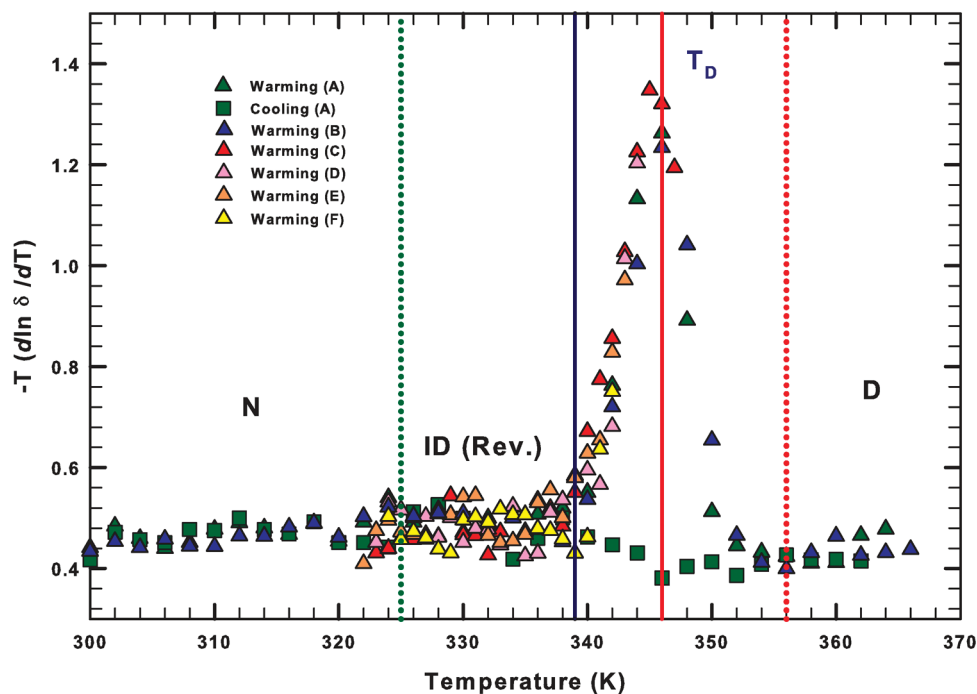
Figure 9. The configurational specific heat evaluated according to the procedure described in eq 3 for all the cycles during the warming phase. The cooling part is reported only for cycle A for simplicity. It is worth noting that the value of the obtained maximum is, within experimental error, the same as that measured by the DSC and TMSC calorimeters.[27]

magnetization intensity nearly the same as that of the warming phase and a second one with a very low intensity value if compared with the first one. A first inspection of this figure reveals essentially two main temperature regions above and

below $T \sim 339$ K, characterized by different behaviors in the contributions I and II.

By cooling, the first contribution I assumes, for a certain T interval inside the D region (up to about 350 K), values close to

those of the warming phase with a similar temperature behavior. For this, we can assume that such a contribution belongs again to the hydration water, whereas the second one, II, belongs to the internal or the water molecules that can be linked to the protein (e.g., solvation water). This latter, as can be seen, is characterized by a progressive increase in its magnetization values by decreasing T. It can also be noticed that whereas the intensity of the contribution II increases by decreasing T, the intensity of contribution I decreases, a situation that is maintained up to ∼339 K; after that, contribution I is characterized by a progressive increase by lowering T. This is accompanied by the evolution of contribution II toward a less intense and stable value. Where I shows the intensity minimum, II is characterized by a broad maximum. During the cooling phase, these two water forms can interact with themselves and with the unfolded protein. In addition, the temperature decreases can cause some configurational instabilities in the biological macromolecule, e.g., a complete or partial unfolding during the first stage of the cooling. This certainly affects the water molecules and thus the I and II species behavior. After that, a restoring of stabilty will start, that as evidenced by Figures 6 and 7 seems to occur at about 340 K where the water ceases to be dominated by free water and are restored bonded structures (like dimers, trimers, and tetramers).

Figure 6 also reports together with the three irreversible cycles A, C, and D the cycles E, F, and G. As said above, cycles E and F that were considered to study the sample annealing are essentially identical: we have operated starting from 320 K with the care to remain inside the region $T \leq 340$ K, reversing the cycle just at this temperature. However, at 330 K, we stopped T, by isothermally annealing for a period of 20 h, inside the N $\rightleftarrows$ ID region in the E case, whereas in the F case the annealing period was of 28 h. During the annealing, the PCS measurements were made in intervals of 1 h. Although these two cycles are identical, we have obtained different results; in the first case (cycle E), after 1 h of the annealing, the denaturation process starts, whereas in the second case the system remains the same for the 28 h in which it was monitored, evidencing no denaturation. In summary, the overall behavior that we observe, regarding the unfolding process, is partially different from that depicted by the calorimetric measurement. We have the same three-state representation, but in our case, we have that the onset of the irreversible denaturation region (D) appears to be located at T_D (in some way, the specific heat maximum marks the ID → D process). However, it appears from the measured data the relevance of the temperature 340 K, that marks the region in which free water essentially plays the main role. The overcoming of such a temperature seems to be the threshold of the N $\rightleftarrows$ ID process, that as evidenced by the cycles E and F may be essentially metastable. Cycle G is instead completely reversible.

Also, the apparent spin—spin relaxation time evolution in the cooling phase (Figure 7B) seems to confirm such an interpretation about the 340 K temperature, located in between a high T region dominated by free water and a low one in which PHB water is the essential component.

In the figure, as it can be seen are plotted the two T_2^* values corresponding to the contributions I and II of the cycles A, C, and D in which the unfolded phase is observed. In the case of cycle A, the T_2^* corresponding to contribution I evidence a maximum just around $T \simeq 340$ K, whereas the one corresponding to contribution II is characterized by a slow evolution toward a stationary behavior at the lowest temperatures. Both these times reach a stable value at about 325 K, i.e., the threshold value of the N $\rightleftarrows$ ID

transition. For the cycles C and D, we observe that the relaxation times corresponding to component II have identical behavior to that of the previously reported cycle, whereas for the component I at the inversion temperature, lower T_2^* values are measured if compared with that of cycle A. However, by decreasing T, this time increases and at about 330 K crosses the values of the previous cycle and evolves at the lowest temperature at the same manner remaining practically constant for $T < 325$ K (going thus inside the protein native region). Such a situation reflects the above-mentioned protein configurational instabilities in the first stage of the cooling phase after the irreversible denaturation.

The isothermal annealing, at $T = 330$ K in cycle E, is illustrated in the upper panel of Figure 7, where the temporal evolution of the two measured contributions is reported. As it can be observed, the temporal behavior of these two spin—spin relaxation times is characterized by a slow evolution to stable values that result nearly the same of the corresponding measured in the irreversible cycles and reported in Figure 7B. From this kinetics, there is the suggestion that the reversible phase may be considered as metastable.

4.2. The Chemical Shift and the Configurational Specific Heat.

Figure 8 illustrates the thermal evolution of the measured ^{1}H NMR chemical shift $\delta(T)$ for all the studied thermal cycles; all data of the warming and cooling phases are considered. In particular, the values corresponding to the spectral contributions I and II observed during the cooling of the samples subject to the irreversible denaturation are also taken into account. For comparison, the data of the pure bulk water chemical shift are also reported.

As it can be observed, both the protein hydration water in the native phase and the bulk liquid chemical shifts are characterized by a linear decrease as the temperature increases. However, the protein hydration water behavior is various and different in the warming and cooling phases. Whereas the warming phase displays an identical temperature evolution of $\delta(T)$ for all the studied cycles, the cooling process is essentially characterized by two main behaviors. In the high temperature regime from 367 to about 350 K, the chemical shift evolves, as a function of T, in the same linear way of the warming phase with about the same values. On the other hand, for $T < 350$ K, the situation changes for the presence of the two spectral contributions I and II, characterizing, as stated above, the system evolution after the irreversible unfolding took place. These contributions are practically identical above T_D, but they evolve separately below it. A very interesting situation marks the warming phase: it is easy to observe in fact a sharp change in $\delta(T)$ that starting at about 339 K stops near 350 K. In addition, if we consider also cycles E and F, whose cooling process starts a few degrees below the onset of that knee, we observe that the corresponding chemical shift increases linearly by decreasing T but parallel to the data measured during the warming phase. This gives a sign that the onset temperature of such a change could be considered as the end of the native state. However, the comparison with the spin—spin relaxation time and the intensity evolution just of these two latter cycles (E and F) suggests that such a temperature is inside a region of metastability where the times of an isothermal annealing can be very long and a warming—cooling cycle is substantially reversible. A very important situation comes out if we consider the analytical continuation of the measured protein hydration water $\delta(T)$, corresponding to the warming phase at the highest temperatures (where essentially all water molecules are free): we observe that such a quantity crosses the pure bulk water chemical

shift at about 370 K (i.e., just near the water boiling temperature). The same situation was found for the NMR self-diffusion coefficient and spin—lattice relaxation time (see Figure 1).

In conclusion, we consider the use of these chemical shifts data to evaluate the configurational specific heat according to the procedure described above (eq 3). Figure 9 shows $(-T\partial\ln\delta(T)/\partial T)_P$ for lysozyme hydration water evaluated from the reported $\delta(T)$ data for the different thermal cycles studied. The $(-T\partial\ln\delta(T)/\partial T)_P$ data obtained during the warming part of the cycles A, B, C, D, E, and F are specifically reported. Only in the case of cycle A we also report the data obtained from the corresponding cooling part; the reason is that practically we have obtained the same results for all the cooling parts of the other cycles. As it can be observed, the value of the obtained maximum is, within the experimental error, the same as that measured by the DSC and TMSC calorimeters.[27] However, there are some differences between the data of these latter experiments and the quantity, obtained according to our procedure, proportional to the constant pressure configurational specific heat $C_{p,\text{conf}}(T)$. This latter one is represented by a narrow and nearly symmetric distribution than that of the endothermic one measured by means of the true calorimetry experiment. A second difference is represented by the values characterizing the high temperature region, $T > 350$ K: whereas in our data these values are about the same, a little lower, of the ones measured in the opposite side of the peak, in the case of the calorimetric experiment the C_p' values are higher in the high T regime with respect to the other ones. In addition, the C_p' measured in the cooling phase is represented by a large peaked distribution centered at about 335 K.

The reason for these differences lies in the fact that the DSC and the TMSC calorimeters measure all the significant system contributions to the specific heat, i.e., the vibrational and configurational parts, whereas here we measure only a contribution proportional to the configurational energies associated with the protein folding. Another important and significative difference is that, whereas in the true calorimetric experiments (like DSC and TMSC) all the contributions to C_p' coming by all the system molecules (lysozyme and water) are macroscopically measured, in our case, we use only the water protons contribution to probe locally the system configurational evolution as a function of the temperature. The first macroscopic canonical approach is certainly more complete (all the energies corresponding to all the available degrees of freedom are evaluated) than this second one local in character. However, in a process in which the physics is essentially governed by configurational changes (like the protein folding process), the latter one, although it furnishes only a quantity proportional to $C_{p,\text{conf}}(T)$, appears to be more useful than the previous one. Therefore, the quantity reported in Figure 9 represents the lysozyme folding process evaluated in terms of microscopic and local configurational changes.

5. CONCLUDING REMARKS

In this paper, we have presented results about the thermal folding of lysozyme in water obtained by means of NMR experiments. We have used the proton NMR FID of the water molecules around the protein as the probe of this complex phenomenon measuring all the related quantities in different thermal cycles by considering protein samples with the same hydration level $h = 0.3$ (a value for which there is about a single monolayer that covers the protein). A hydration condition that, as widely recognized, represents a threshold value for the protein biological

activity[6−8] and for which the water can be used as a monitor for the protein changes under thermal perturbations.[8−10,12,14,28] We have followed the suggestions of a previous calorimetric study[27] whose findings, by exploring the water—lysozyme system in proper thermal cycles, indicate that the protein denaturation takes place by considering the macromolecule in terms of a three-stage model: a native structure (compact and globular) that evolves in an intermediate state (globular, open, or molten) through a reversible transition and finally in the irreversible denatured state as an essentially unfolded polymer chain (a sort of disordered coil). Thus, a progressive conformational change occurs from the native globular structure to that of an open coil in which the protein interactions are switched off, and the macromolecular packing decreases at each of the steps characterizing the entire $N \rightleftharpoons ID \rightarrow D$ process.

The actual literature,[10,12,14] especially the theoretical,[4,13,21,23,24,31,32] gives the idea that in all these stages of folding and unfolding processes water certainly plays a role; however, we do not have definitive answers to this important question on molecular based experiments. Thus, here by means of an NMR study we have considered two aspects like the monitoring of the protein structural changes and the verification of the possible manners in which water contributes to the protein denaturation.

The obtained results, by confirming that the local probe "water" accurately follows all the protein changes in the warming and cooling phases of the thermal cycles used to explore the thermal denaturation of the lysozyme, also indicate that some water physical properties, especially the HB, appear to be at the origin of the studied phenomenon.

We have started by considering previous experimental results, in the same system: the water self-diffusion coefficient and the vibrational OH-stretching measured, respectively, by means of the NMR and FTIR spectroscopy. Whereas the first experiment suggests a dynamical crossover just at the temperature of the onset of the irreversible denatured phase (D) observed by the calorimetric experiments, the second experiment gives evidence that such crossover temperature marks the borderline of a region in which the not bonded free water represents the larger moiety. With the D_S being related, by means of the Adam—Gibbs model, to the configurational entropy and with the hydration water concentration being enough to cover the protein surface, we argued that the water molecules have to follow the changes in the protein structure.

Making reference to these findings, we have extracted from the NMR proton spectra the intensity (the molecular magnetization) and the apparent spin—spin relaxation time. Both of these quantities evidence that protein water not only follows all three stages of the denaturation process but also reveal the active role of water, essentially in the intermediate reversible stage, in the protein denaturation. From the comparison with the OHS vibrational spectra measured by means of the FTIR spectroscopy, we have an indication that the two changes in the $N \rightleftharpoons ID \rightarrow D$ regions are related to corresponding changes in the water structure from the region dominated by the NHB and PHB water forms to a final situation (irreversible denaturation) where the water monomers are dominant.

We also observe that, whereas in the warming phase of the proposed thermal cycles, up to the onset of the irreversible denaturation the thermal evolution of the system is well monitored by the hydration water (the only that contributes to the NMR FID) when the irreversible structural change of the biomolecule starts, a new contribution due to the protein internal water appears. This form of water, which is hydrogen bonded to

14292

dx.doi.org/10.1021/jp205285t |J. Phys. Chem. B 2011, 115, 14280–14294

the folded protein internal sites, at this stage can recover its degrees of freedom and thus contributes to the NMR spectra. During the heating phase, significant changes appear in the $I_{NMR}(T)$ and the $T_2^*(T)$ data at all the temperatures marking the crossovers of the three unfolding stages. Instead, in the cooling phase after the protein denaturation, a different physical scenario is observed: now the macromolecule is an open random coil and the water molecules evolve in a different way with respect to the previous case of a rigid and dense globular structure. In the actual situation, the protein offers to the water all its hydrophilic and hydrophobic groups. At the same time, a temperature decrease can also cause some configurational changes in the biopolymer toward a more dense structure induced by entropic effects as far as in any polyelectrolyte dissolved in a solvent.[47]

Although the protein is now in a denatured state, all the molecular ingredients that in principle can originate a new folding process are again present in this concentrated protein—water suspension. This in our opinion explains what happens during the cooling phase of the denatured protein when the behaviors of the corresponding magnetizations and relaxation times can be expressed in terms of two spectral contributions, I and II, characterizing the water suspension of these unfolded disordered coils.

As it can be observed in Figures 6B and 7B, there are in this phase two distinct regions: one more dynamical and "unstable" at the highest temperatures near the irreversible denaturation temperature and a second in which the system relaxes in a more stable, nearly temperature independent, physical configuration.

Moreover, the proton chemical shift frequency $\delta(T)$ and its derivative $(-T\partial \ln \delta(T)/\partial T)_P$ related, respectively, to the configurational entropy and the corresponding specific heat confirm how water marks the entire thermal evolution of the system under study. There is in these data a complete agreement with all the findings of the previous experiments performed under the same conditions, in particular with the NMR self-diffusion, the quasi-elastic neutron scattering relaxation time, for which the configurational entropy (Figure 8) can give a proper description of the system. Just in such a quantity, we observe a marked change in the temperature interval 339 K < T < 350 K. In addition, just after this latter temperature, the protein irreversibly denatures and the proton $\delta(T)$ (representing now the chemical shift of a mixture of both the hydration and protein internal water) evolves toward the corresponding value of the bulk water that crosses at about 370 K. In addition, on looking at Figure 8 during the warming cycle, the temperature 339 K seems to be the locus where the protein native state in our protein suspension ceases to exist.

Finally, we have comparatively considered our obtained configurational specific heat (Figure 9) with the one observed in the calorimetric experiments.[27] Although the results on the $C_p(T)$ characterized by a marked maximum at about the same temperature T_D (~346 K) are similar, we have confirmation that all the unfolding process is due exclusively to changes in the system configurational degrees of freedom.

■ AUTHOR INFORMATION

Corresponding Author

*E-mail: francesco.mallamace@unime.it.

■ ACKNOWLEDGMENT

■ REFERENCES

(1) Angell, C. A. In *Water: a Comprehensive Treatise*; Franks, F., Ed.; Plenum: New York, 1982; Vol. 7, pp 1—81.

(2) Mishima, O.; Stanley, H. E. *Nature* **1998**, *396*, 329.

(3) Debenedetti, P. G.; Stanley, H. E. *Phys. Today* **2003**, *56*, 40.

(4) Fersht, R. A. *Structure and Mechanism in Protein Science: A Guide to Enzyme Catalysis and Protein Folding*; W.H. Freeman and Co.: New York, 1999.

(5) Ball, P. *Chem. Rev.* **2008**, *108*, 74–108.

(6) Rupley, J. A.; Careri, G. *Adv. Protein Chem.* **1991**, *41*, 37.

(7) Rupley, J. A.; Yang, P. H.; Tollin, G. Water in Polymers. *ACS Symp. Ser.* **1980**, *127*, 111.

(8) Zaccai, G. *Philos. Trans. R. Soc., B* **2004**, *359*, 1269–1275.

(9) Parak, F.; Knapp, E. W. *Proc. Natl. Acad. Sci. U.S.A.* **1984**, *81*, 7088.

(10) Doster, W.; Kusak, S.; Petry, W. *Nature* **1989**, *337*, 754. *Phys. Rev. Lett.* **1990**, *65*, 1080.

(11) Parak, F. *Rep. Prog. Phys.* **2003**, *66*, 103.

(12) Fenimore, P. W.; Frauenfelder, H.; McMahon, B. H.; Parak, F. G. *Proc. Natl. Acad. Sci. U.S.A.* **2002**, *99*, 16047.

(13) Smith, J.; Kuczera, K.; Karplus, M. *Proc. Natl. Acad. Sci. U.S.A.* **1990**, *87*, 1601.

(14) Doster, W.; Bachleitner, A.; Dunau, R.; Hiebl, M.; Lüscher, E. *Biophys. J.* **1986**, *50*, 213.

(15) Mallamace, F.; Chen, S.-H.; Broccio, M.; Corsaro, C.; Crupi, V.; Venuti, V.; Majolino, D.; Baglioni, P.; Fratini, E.; Vannucci, C.; Stanley, H. E. *J. Chem. Phys.* **2007**, *127*, 045104.

(16) Errington, J. R.; Debenedetti, P. G. *Nature (London, U. K.)* **2001**, *409*, 318.

(17) Mallamace, F.; Broccio, M.; Corsaro, C.; Faraone, A.; Majolino, D.; Venuti, V.; Liu, L.; Mou, C.-Y; Chen, S.-H. *Proc. Natl. Acad. Sci. U.S.A.* **2007**, *104*, 424–428.

(18) The experimental proof on the existence of the low density water network is due to the onset at room temperature of a spectral contribution in the OH stretching spectra centered at about 3120 cm^{-1} that on decreasing the temperature evolves towards the low density amorphous water (the so-called LDA phase). We stress that such a new contribution is independent of any isosbestic point; in particular, it excludes the presence of this "special point" in water from the ambient to the supercooled regime.

(19) Poole, P. H.; Sciortino, F.; Essmann, U.; Stanley, H. E. *Nature* **1992**, *360*, 324.

(20) Chen, S. H.; Liu, L.; Fratini, E.; Baglioni, P.; Faraone, A.; Mamontov, E. *Proc. Natl. Acad. Sci. U.S.A* **2006**, *103*, 9012.

(21) Kumar, P.; Yan, Z.; Xu, L.; Mazza, M. G.; Buldyrev, S. V.; Chen, S. H.; Sastry, S.; Stanley, H. E. *Phys. Rev. Lett.* **2006**, *97*, 177802.

(22) Kauzmann, W. *Adv. Protein Chem.* **1959**, *14*, 1.

(23) Frauenfelder, H.; Petsco, G. A.; Tsernoglou, D. *Nature* **1979**, *260*, 558.

(24) Anfinsen, C. *Science* **1973**, *181*, 223.

(25) Hameed, M.; Ahmad, B.; Fazili, K. M.; Andrabi, K.; Khan, R. H. *J. Biochem.* **2007**, *141*, 573.

(26) Smeller, L.; Meersman, F.; Heremans, K. *Biochim. Biophys. Acta* **2006**, *1764*, 497.

(27) Salvetti, G.; Tombari, E.; Mikheeva, L.; Johari, G. P. *J. Phys. Chem. B* **2002**, *106*, 6081.

(28) Hedoux, A.; Ionov, R.; Willart, J.-F.; Lerbret, A.; Affouard, F.; Guinet, Y.; Descamps, M.; Prevost, D.; Paccou, L.; Danede, F. *J. Chem. Phys.* **2006**, *124*, 014703.

(29) Green, J. L.; Fan, J.; Angell, C. A. *J. Phys. Chem.* **1994**, *98*, 13780.

(30) Lee, R. C.; Despa, F.; Guo, L.; Betala, P.; Kuo, A.; Thiyagarajan, P. *Ann. Biomed. Eng.* **2006**, *34*, 1190.

(31) Kobayashi, Y.; Wako, H.; Saito, N. *J. Phys. Soc. Jpn.* **2007**, *76*, 074802.

14293

dx.doi.org/10.1021/jp205285t |*J. Phys. Chem. B* 2011, 115, 14280–14294

(32) Mark, A. E.; van Gunsteren, W. F. *Biochemistry* **1992**, *31*, 7745.

(33) Zhang, Y.; Lagi, M.; Liu, D.; Mallamace, F.; Fratini, E.; Baglioni, P.; Mamontov, E.; Hagen, M.; Chen, S. H. *J. Chem. Phys.* **2009**, *130*, 135101.

(34) Mallamace, F.; Corsaro, C.; Broccio, M.; Branca, C.; Gonzalez-Segredo, N.; Spooren, J.; Chen, S.-H.; Stanley, H. E. *Proc. Natl. Acad. Sci. U.S.A.* **2008**, *105*, 12725–12729.

(35) Suresh, S. J.; Naik, V. M. *J. Chem. Phys.* **2000**, *113*, 9727.

(36) Lagi, M.; Chu, X.; Kim, C.; Mallamace, F.; Baglioni, P.; Chen, S.-H. *J. Phys. Chem. B* **2008**, *112*, 1571.

(37) Bloembergen, N.; Purcell, E. M.; Pound, R. V. *Phys. Rev.* **1948**, *73*, 679.

(38) Adam, G.; Gibbs, J. H. *J. Chem. Phys.* **1965**, *43*, 139.

(39) Matubayasi, M.; Wakai, C.; Nakahara, M. *Phys. Rev. Lett.* **1997**, *78*, 2573–2576.

(40) Modig K, K.; Pfrommer, B. G.; Halle, B. *Phys. Rev. Lett.* **2003**, *90*, 075502.

(41) Sebastiani, D.; Parrinello, M. *Phys. Chem. Chem. Phys.* **2002**, *3*, 675–679.

(42) Lindon, J. C.; Beckonert, O. P.; Holmes, E.; Nicholson, J. K. *Prog. Nucl. Magn. Reson. Spectrosc.* **2009**, *55*, 79–100.

(43) Purcell, E. M.; Torrey, H. C.; Pound, R. V. *Phys. Rev.* **1946**, *69*, 37.

(44) Bloch, F. *Phys. Rev.* **1946**, *70*, 460.

(45) Becker, E. D. In *Encyclopedia of Nuclear Magnetic Resonance*; Grant, D. M., Harris, R. K., Eds.; Wiley: Chichester, U.K., 1996; p 2409.

(46) Abragam, A. *The Principles of Nuclear Magnetism*; Clarendon: Oxford, U.K., 1961.

(47) de Gennes, P.-G. *Scaling Concepts in Polymer Physics*; Cornell Univ. Press: Ithaca, NY, 1979.

14294

dx.doi.org/10.1021/jp205285t |*J. Phys. Chem. B* 2011, 115, 14280–14294